A Fast Low-Rank Matrix Factorization Method for Dynamic Magnetic Resonance Imaging Restoration

Fei Xu[a*], Jingjing Zhang[a], Yanmei Shi[a], Kaixin Kang[a] and Shuguo Yang[a]
[a] *College of Mathematics and Physics*
[a] *Qingdao University of Science and Technology*
[a] *Qingdao 266061, China*
Email: xf_em@163.com; m17863974117@163.com; 13165150979@163.com; 13012405685@163.com; ysg_2005@163.com
* *Corresponding Author*

***Abstract*—Nowadays, over 90 percent of the medical data comes from the medical image. People can reduce the medical faults in diagnoses by using computer to analyze and process these medical image data. In this paper, we focus on the reconstruction of dynamic magnetic resonance imaging (MRI), which is crucial to medical diagnoses. Considering the successful application of the robust principal component analysis (RPCA) in MRI to increase the imaging speed and improve the imaging quality, we propose a model based on RPCA. However, the conventional models based on RPCA have two drawbacks: one is that the nuclear norm is often inexact rank approximation, especially when there exist some large singular values; the other is that dealing with the whole data matrix is always time consuming. Our strategies are to adopt a more exact nonconvex rank approximation and matrix factorization, respectively. The former has been proved to be better than the nuclear norm, while the latter can reduce computation complexity by turning the computing object into a core matrix, which is much smaller than the original data matrix. Then the alternating direction method (ADM) is used to solve the well-designed model. Experiments of cardiac cine and abdomen MRI data are conducted to verify the superior performance of our method in both image clarity and computation efficiency when compared with the conventional MRI reconstruction methods.**

***Keywords*-Magnetic resonance imaging; nonconvex; low-rank plus sparse; low-rank matrix factorization.**

I. Introduction

Dynamic magnetic resonance imaging (dMRI) plays an important role in medical diagnosis and medical research for the reason that it can provide static and dynamic image data on the structure and function of the assessed organs such as the heart, liver, abdomen and so on [1], [2], [3]. However, it is difficult for the patient to lay still and hold breath during the imaging, hence, the low imaging speed limits to obtain spatial and temporal resolution when imaging the moving organs. For this reason, it is urgent to overcome this limitation by some techniques so as to accelerate the reconstruction of MRI.

There have been many methods proposed to address this issue, for example, parallel imaging [4], compressed sensing [5] and k-t acceleration [6]. Considering these multiple temporal images are slowly changing and highly coherent, they have natural low-rank structure until damage occurs to induce sparse components, hence, there emerge some methods based on low-rank and sparse decomposition: Otazo *et al.* [2] applied a low-rank plus sparse matrix decomposition model to reconstruct undersampled dynamic MRI as a superposition of background and dynamic components in various medical imaging problems including cardiac perfusion, cardiac cine and so on; Zonoobi *et al.* [7] utilized some priori knowledge for the low-rank and sparse matrix decomposition to fast reconstruct the dynamic 3D MR images from undersampled k-space data; Zhong *et al.* [8] employed a low-rank plus sparse model by dictionary learning to reconstruct 3D MRI with better performance; Roohi *et al.* [9] proposed a low-rank plus sparse tensor decomposition model to realize the reconstruction of MRI by solving the related optimization with the alternating direction method of multipliers (ADMM). Christodoulou *et al.* [10] integrated parallel imaging, low-rank modeling and sparse modeling to improve cardiovascular MRI. Gao *et al.* [11] proposed a phase-constrained low-rank model for reconstruction of Diffusion-weighted MRI images.

In theory, general RPCA recovers the low-rank part and sparse part by convex method, i.e., using nuclear norm as the approximation of the rank of low-rank matrix. However, this method gets into trouble because nuclear norm cannot approximate the rank function well, which we have discussed in our previous work [12]. In this paper, we propose a low-rank and sparse scheme for reconstruct dMRI by integrating the nonconvex rank approximation and low-rank matrix factorization. Concretely, we use logdet function as the rank approximation and factorize the low-rank matrix into three parts including a small core matrix wherein. Hence, our method only needs the singular value decomposition (SVD) of a thin matrix, which improves the imaging speed greatly.

The remainder of this paper is organized as follows. Section II presents the related models and algorithm in detail. Experimental results are described and analyzed in Section III and Section IV draws the conclusion.

978-1-7281-4024-7/19/$31.00 ©2019 IEEE
DOI 10.1109/BIGCOM.2019.00014

II. Models and Algorithm

In this section, we introduce our model which is not only based on low-rank and sparse, but also adopts the strategy of matrix factorization. Then, we propose our algorithm using augmented Lagrangian multiplier (ALM) method to solve the associated rank minimization problem.

A. Models

The low-rank plus sparse representation model of dMRI in [2] is as follows:

$$\min_{L,S} \|L\|_* + \lambda\|TS\|_1 \quad \text{s.t.} \quad E(L+S) = d, \tag{1}$$

where $L, S \in \mathbf{C}^{m\times n}$, T is a sparsifying transform for S, E is the encoding or acquisition operator and d is the undersampled k-t data.

By using regularization rather than strict constraints, the unconstrained formulation of (1) is as follows:

$$\min_{L,S} \frac{1}{2}\|E(L+S) - d\|_2^2 + \lambda_1\|L\|_* + \lambda_2\|TS\|_1, \tag{2}$$

where λ_1 and λ_2 are trade off parameters used to balance the data consistency versus the complexity of the solution.

For problem (2), on the one hand, we adopt the following logdet function as a better rank approximation [13] to replace the nuclear norm $\|L\|_*$,

$$\|L\|_{ld} = \log\ \det(I + (L^TL)^{\frac{1}{2}}) = \sum_{i=1}^{\min\{m,n\}} \log(1+\sigma_i^L). \tag{3}$$

On the other hand, we use matrix factorization which is useful in high dimensional data processing. In this paper, the low-rank part L is factorized as

$$L = UCV^T, \tag{4}$$

where $U \in \mathbf{R}^{m\times k}$, $C \in \mathbf{R}^{k\times k}$, $V \in \mathbf{R}^{n\times k}$, $k \ll \min\{m,n\}$, $U^TU = I$ and $V^TV = I$, I is the identity matrix with appropriate dimension.

Based on the orthogonal property of U and V, we can easily derive the following formula:

$$\begin{aligned}\|L\|_{ld} &= \log\ \det(I + (VC^TU^TUCV^T)^{\frac{1}{2}}) \\ &= \text{logdet}(I + V(C^TC)^{\frac{1}{2}}V^T)) \\ &= \log\ \det(I + (C^TC)^{\frac{1}{2}})) = \|C\|_{ld}.\end{aligned} \tag{5}$$

Obviously, the factorization $L = UCV^T$ may be used so as to avoid the SVD for a large matrix.

Overall, our model finally reduces to the following form:

$$\begin{aligned}&\min_{U,C,V,S} \frac{1}{2}\|E(UCV^T + S) - d\|_2^2 + \lambda_1\|C\|_{ld} + \lambda_2\|TS\|_1 \\ &\text{s.t.} \quad U^TU = I, \qquad V^TV = I.\end{aligned} \tag{6}$$

B. Algorithm

By setting the initial values $L = M = E^Hd, S = 0$, we solve (6) by the following six steps to update all the variables at each iteration.

1) Updating S: For the $S-$update, we can resort to the data consistency strategy [2], which uses the singular value soft-thresholding operator of TS. Then, the $S-$update for (6) is as follows:

$$S = T^{-1}(\Lambda_{\lambda_2}(T(M-L))), \tag{7}$$

where the matrix M is used to maintain data consistency.

2) Updating U: The subproblem for optimizing U is

$$\min_{U^TU=I} \|UC - \Theta V\|_F^2, \tag{8}$$

where $\Theta = (E^HE)^{-1}E^Hd - S$, utilizing the solution of classical orthogonal Procrustes problem [14], we have

$$U = \mathcal{L}(\Theta VC^T)(\mathcal{R}(\Theta VC^T))^T, \tag{9}$$

where $\mathcal{L}(Z)$ and $\mathcal{R}(Z)$ are the left and right singular vectors of Z, respectively.

3) Updating V: The subproblem for optimizing V is

$$\min_{V^TV=I} \|VC^T - \Theta^TU\|_F^2, \tag{10}$$

similar to the $U-$update, we have

$$V = \mathcal{L}(\Theta^TUC)(\mathcal{R}(\Theta^TUC))^T, \tag{11}$$

4) Updating C: The subproblem of optimizing C is

$$\min_C \lambda_1\|C\|_{ld} + \frac{1}{2}\|U^T\Theta V - C\|_F^2, \tag{12}$$

by using the singular value shrinkage operator [15],

$$C = \mathcal{F}_{\lambda_1}(U^T\Theta V), \tag{13}$$

where $\mathcal{F}_\tau(Z) = \mathcal{L}(Z)\text{diag}(\max(0, \sigma_i^Z - \tau))(\mathcal{R}(Z))^T$.

5) Updating L: By the results of (9)(11)(13), we have

$$L = UCV^T. \tag{14}$$

6) Updating M: The matrix M is obtained to maintain data consistency. By applying the shrinkage operator to $M-L$ at the last iteration, we obtain $M-$update as follows:

$$M = L + S - E^H(E(L+S) - d). \tag{15}$$

In (15), the aliasing artifacts corresponding to the residual $E^H(E(L+S)-d)$ are subtracted from $L+S$.

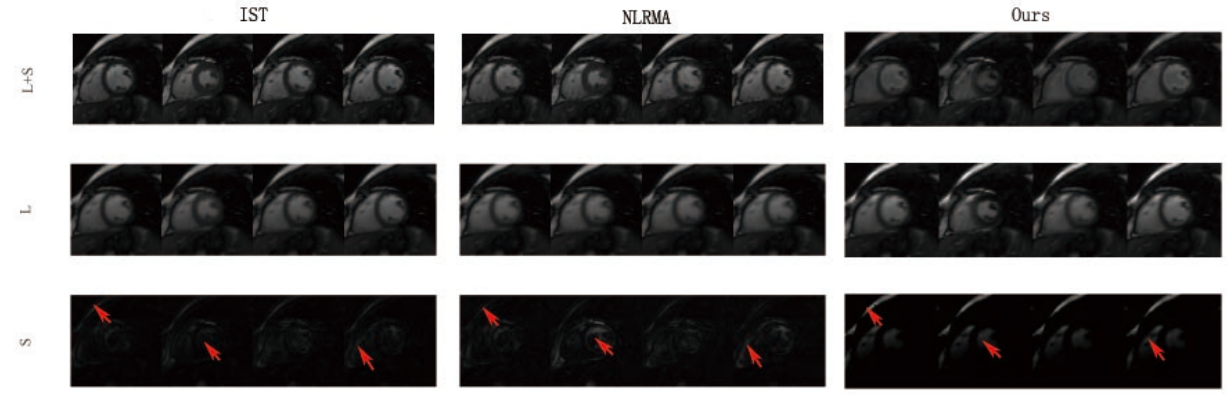

Figure 1: Performance of different algorithms for dynamic cardiac cine. The three columns from left to right correspond to: IST[2], NLRMA[12] and Ours; the three rows from top to bottom correspond to $L+S$, low-rank component L and sparse component S of the observed data D. This figure can be better viewed in zoomed PDF.

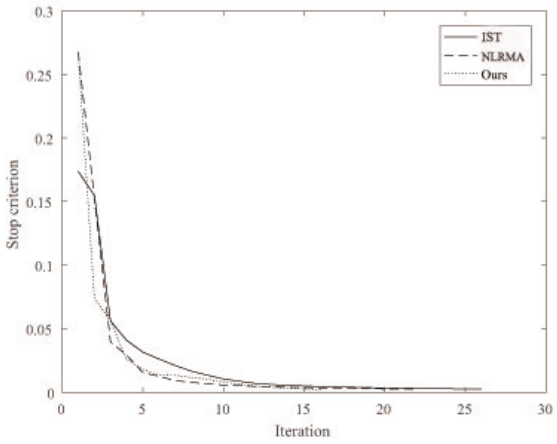

Figure 2: Convergence curves with respect to iterations for cardiac cine data by three different methods IST[2], NLRMA[12] and Ours.

III. Experimental Results and Discussion

In this section, firstly, we compare our proposed algorithm with IST[2] and NLRMA[12] for dynamic cardiac cine data; then, we compare our method with several current methods including k-t SENSE[16], XD-GRASP[17] and IST[2] for dynamic abdomen data. All the data sets we used can be downloaded online at http://cai2r.net/resources/ software/ls-reconstruction-matlab-code. Our numerical experiments are run in MATLAB R2013a on a PC with a COREi3 2.40GHz CPU and 4GB memory.

Our algorithm stops when the relative error is less than 2.5×10^{-3}, namely,

$$\text{RelErr} = \frac{\|L_{k+1} + S_{k+1} - (L_k + S_k)\|_F}{\|L_k + S_k\|_F} \leq 2.5 \times 10^{-3}, \tag{16}$$

Futhermore, we compute the root mean square error (RMSE) defined as:

$$\text{RMSE} = \frac{\|D - L - S\|_F}{\|D\|_F}\ , \tag{17}$$

where D, L, S represent the observed data, low-rank and sparse matrices, respectively.

A. Dynamic Cardiac Cine

We choose $\lambda_1 = 1000, \lambda_2 = 0.2$ on dynamic cardiac cine data. Our experimental results compared with the other two algorithms (IST[2] and NLRMA[12]) are showed in Fig. 1, the selected image size is $128 \times 128 \times 40$, the display window is $[0, 1]$. Fig. 2 shows that our method converges earlier and faster. Besides the comparable visual effects, our method has improvements by decreasing the computation time around 10% to 20% when compared with the other two, as shown in Table I. Especially, our main experimental quantitative indicators, such as RMSE and relative error, have reduced greatly.

Table I: **COMPUTATIONAL RESULTS FOR DYNAMIC CARDIAC CINE**

Algorithm	Time(s)	Iteration	RMSE	Relative Error
IST	190.7	26	0.5063	$2.47 * 10^{-3}$
NLRMA	178.8	22	0.4829	$2.42 * 10^{-3}$
Ours	153.8	16	0.2338	$2.18 * 10^{-3}$

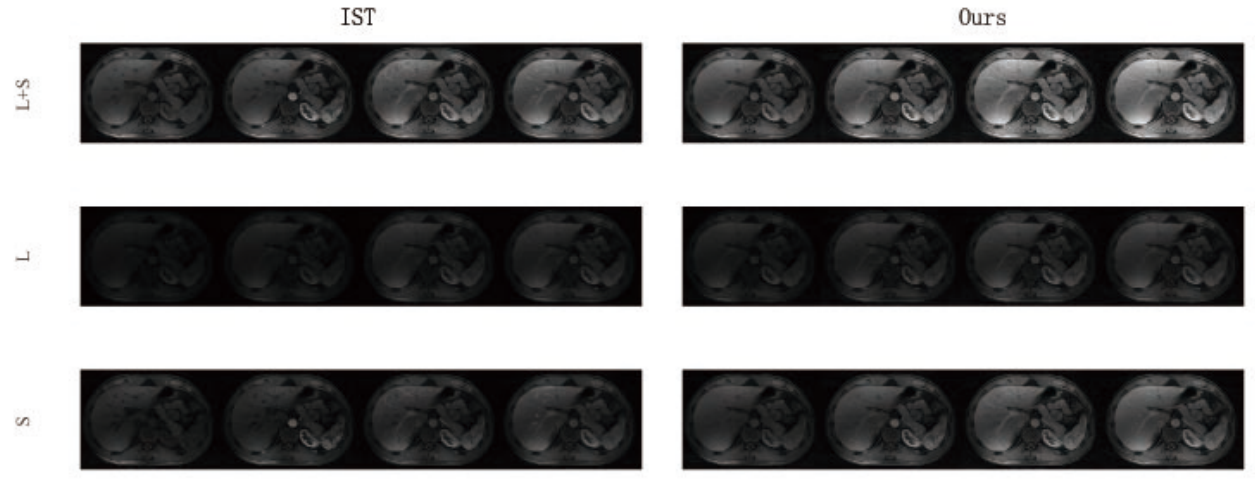

Figure 3: Performance of different algorithms for dynamic abdomen. The two columns from left to right correspond to: IST[2] and Ours; the three rows from top to bottom correspond to $L + S$, low-rank component L and sparse component S of the observed data D. This figure can be better viewed in zoomed PDF.

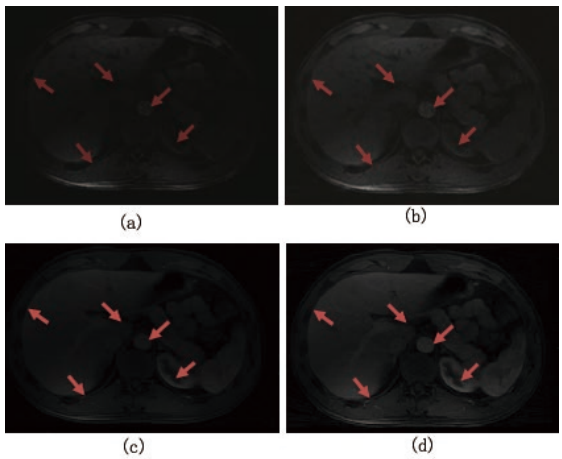

Figure 4: Reconstruction results of four algorithms for the dynamic abdomen: (a) k-t SENSE[16], (b) XD-GRASP[17], (c) IST[2], (d) Ours.

B. Dynamic Abdomen

1) Compare the abdominal $L+S$, L and S: We compare our algorithm with IST[2] by using the abdominal data. Here, we choose $\lambda_1 = 10000$, $\lambda_2 = 0.5$. Fig. 3 demonstrates the comparison of the low-rank part L, the sparse part S and the reconstructed $L+S$ part of the abdomen data by the two algorithms IST[2] and Ours when reaching the same relative error; Table. II reflects the comparison of the indicators, including the running time, the times of iterations and the RMSEs. It can be obviously seen that our algorithm is more efficient.

Table II: **COMPUTATIONAL RESULTS FOR DYNAMIC ABDOMEN**

Algorithm	Time(s)	Iteration	RMSE
IST	1505.84	50	11.4246
Ours	250.98	5	3.9073

2) Compare the abdominal L: We compare the experimental results among our method and there different methods k-t SENSE[16], XD-GRASP[17] and IST[2]. Fig. 4 shows the comparisons of the different reconstruction results when the parameters $\lambda_1 = 10000, \lambda_2 = 0.5$. Note the spots which several red arrows point to. Table III lists the comparisons of RMSE and running time among these four algorithms. Our method has obvious advantage over the other three.

Table III: **COMPARISONS OF RUNNING TIME AND RMSE FOR DYNAMIC ABDOMEN**

	k-t SENSE	XD-GRASP	IST	Ours
Time(s)	336.2	310.3	1505.84	250.98
RMSE	12.4521	11.7607	9.2530	3.9073

IV. Conclusion

In this paper, we propose a low-rank and sparse formulation and integrate nonconvex rank approximation and matrix factorization for reconstructing dynamic magnetic resonance imaging. The comparisons with other current methods obviously show that our algorithm greatly speeds up the MRI

reconstruction. This may be due to two reasons, one is that we use the logdet function as the rank approximation which is more exact than the traditional nuclear norm as the rank approximation, the other reason is that the low-rank matrix in our model is factorized into three smaller parts, so the time consuming singular value decomposition (SVD) on the original large matrix can be avoided. Experiments are performed using dynamic cardiac cine data and abdomen data, we find that our algorithm not only greatly shortens the running time, but also improves the reconstruction effects. In our future work, we will consider the MRI data as a tensor rather than a matrix in order to use the linear relationship between the different frames along the time mode.

ACKNOWLEDGMENT

This work was supported by the Science and Technology Project of Colleges and Universities in Shandong Province under Grant No. J18KA314, the Original Innovation Project in Qingdao City under Grant 18-2-2-64-jch, and the Undergraduate Innovation and Entrepreneurship Training Program, Qingdao University of Science and Technology No. 201810426201.

At last, the authors would like to thank Dr. Yongyong Chen of University of Macau and Dr. Chong Peng of Qingdao University for giving really professional suggestions that have helped to improve the quality of this paper.

REFERENCES

[1] L. Axel and R. Otazo, "Accelerated MRI for the assessment of cardiac function," Brit. J. of Radiol., vol. 89, no. 1063, pp. 20150655, 2016.

[2] R. Otazo, E. J. Candes, and D. Sodickson, "Low-rank plus sparse matrix decomposition for accelerated dynamic MRI with separation of background and dynamic components," Magn. Reson. Med., vol. 73, no. 3, pp. 1125-1136, Mar. 2015.

[3] L. Chen, B. Yang and X. Wang, "Dynamic Magnetic Resonance Imaging Reconstruction Based on Nonconvex Low-Rank Model," Math. Probl. Eng., vol. 2017, Article ID 9576950, 11 pages, 2017.

[4] K. P. Pruessmann, M. Weiger, M. B. Scheidegger and P. Boesiger, "SENSE: sensitivity encoding for fast MRI," Magn. Reson. Med., vol. 42, no.5, pp. 952-962, Nov. 1999.

[5] M. Lustig, D. L. Donoho and J. M. Pauly, "Sparse MRI: The Application of Compressed Sensing for Rapid MR Imaging," Magn. Reson. Med., vol. 58, no. 6, pp. 1182-1195, Dec. 2007.

[6] J. Tsao and S. Kozerke, "MRI temporal acceleration techniques," J. Magn. Reson. Imaging, vol. 36, no. 3, pp. 543-560, 2012.

[7] D. Zonoobi, S. F. Roohi and A. A. Kassim, "Low-Rank and Sparse Matrix Decomposition with a-priori knowledge for Dynamic 3D MRI reconstruction," Clin. Orthop. Relat. R., arxiv: 1411.6206, 2014.

[8] W. Zhong, D. Li, L. Wang and M. Zhang, "Low-rank plus sparse reconstruction using dictionary learning for 3D-MRI," in International Congress on Image and Signal Processing, BioMedical Engineering and Informatics (CISP-BMEI'16), Datong, China, Oct. 2016, pp. 1407-1411.

[9] S. F. Roohi, D. Zonoobi, A. A. Kassim and J. L. Jaremko, "Dynamic MRI reconstruction using low rank plus sparse tensor decomposition," in IEEE International Conference on Image Processing (ICIP'16), Phoenix, AZ, USA, Sept. 2016, pp. 1769-1773.

[10] A. G. Christodoulou, H. Zhang, B. Zhao, T. K. Hitchens, C. Ho and Z. P. Liang, "High-Resolution Cardiovascular MRI by Integrating Parallel Imaging With Low-Rank and Sparse Modeling," IEEE Trans. Biomed. Eng., vol. 60, no. 11, pp. 3083-3092, Nov. 2013.

[11] H. Gao, L. Li, K. Zhang, W. Zhou and X. Hu, "PCLR: Phase-Constrained Low-Rank Model for Compressive Diffusion-Weighted MRI," Magn. Reson. Med., vol. 72, no. 5, pp. 1330-1341, Nov. 2014.

[12] F. Xu, J. Han, Y. Wang, M. Chen, Y. Chen, G. He and Y. Hu, "Dynamic Magnetic Resonance Imaging via Nonconvex Low-Rank Matrix Approximation," IEEE Access, vol. 5, pp. 1958-1966, 2017.

[13] C. Peng, Z. Kang, M. Yang and Q. Cheng, "Feature Selection Embedded Subspace Clustering," IEEE Signal Process. Lett., vol. 23, no. 7, pp. 1018-1022, Jul. 2016.

[14] P. H. Schnemann, "A generalized solution of the orthogonal procrustesproblem," Psychometrika, vol. 31, no. 1, pp. 1-10, Mar. 1966.

[15] J. F. Cai, E. J. Candes and Z. Shen, "A singular value thresholding algorithm for matrix completion," SIAM J. Optim., vol. 20, no. 4, pp. 1956-1982, 2010.

[16] J. Tsao, P. Boesiger, and K. P. Pruessmann, "k-t blast and k-t sense: Dynamic MRI with high frame rate exploiting spatiotemporal correlations," Magn. Reson. Med., vol. 50, no. 5, pp. 1031-1042, 2003.

[17] L. Feng, R. Grimm, and K. T. O. B. et al., "Golden-angle radial sparse parallel MRI: combination of compressed sensing, parallel imaging, and golden-angle radial sampling for fast and flexible dynamic volumetric MRI," Magn. Reson. Med., vol. 72, no. 3, pp. 707-717, 2014.